NAVAL POSTGRADUATE SCHOOL
Monterey, California

THESIS

MODELING TRANSIENT THERMAL BEHAVIOR
IN A THRUST VECTOR CONTROL JET VANE

by

Margaret Mary Reno

December 1988

Thesis Advisor: R. H. Nunn

REPORT DOCUMENTATION PAGE

a REPORT SECURITY CLASSIFICATION NCLASSIFIED	1b RESTRICTIVE MARKINGS
a. SECURITY CLASSIFICATION AUTHORITY	3 DISTRIBUTION / AVAILABILITY OF REPORT Approved for public release; distribution is unlimited
b DECLASSIFICATION / DOWNGRADING SCHEDULE	
PERFORMING ORGANIZATION REPORT NUMBER(S)	5 MONITORING ORGANIZATION REPORT NUMBER(S)
a NAME OF PERFORMING ORGANIZATION aval Postgraduate School 6b OFFICE SYMBOL (If applicable) Code 69	7a NAME OF MONITORING ORGANIZATION
c. ADDRESS (City, State, and ZIP Code) Monterey, California 93943-5000	7b ADDRESS (City, State, and ZIP Code) Monterey, California 93943-5000
a. NAME OF FUNDING / SPONSORING ORGANIZATION 8b OFFICE SYMBOL (If applicable)	9 PROCUREMENT INSTRUMENT IDENTIFICATION NUMBER
c. ADDRESS (City, State, and ZIP Code)	10 SOURCE OF FUNDING NUMBERS PROGRAM ELEMENT NO / PROJECT NO / TASK NO / WORK UNIT ACCESSION NO

1. TITLE (Include Security Classification)

odeling Transient Thermal Behavior in a Thrust Vector Control Jet Vane

2. PERSONAL AUTHOR(S)

RENO, Margaret M.

3a. TYPE OF REPORT	13b TIME COVERED	14 DATE OF REPORT (Year, Month, Day)	15 PAGE COUNT
aster's Thesis	FROM _____ TO _____	1988 December	48

6. SUPPLEMENTARY NOTATION

he views expressed in this thesis are those of the author and do not reflect the official olicy or position of the Department of Defense or the U. S. Government

7 COSATI CODES			18 SUBJECT TERMS (Continue on reverse if necessary and identify by block number)
FIELD	GROUP	SUB-GROUP	Thrust Vector Control Jet Vane, TVC, STARS, Jet Vane

9. ABSTRACT (Continue on reverse if necessary and identify by block number)

An attempt was made to model the transient thermal response of jet vanes used for hrust control. A simple computer model based on lumped capacitance methods using boundary ayer convection and stagnation point heating as thermal inputs appeared to adequately redict temperatures for a quarter-scale model. This report details the attempt to enlarge he model to allow comparison between thermal predictions and the results of tests on a ull-scale prototype jet vane. It was determined that the model could not be considered a hermal representation of the full-scale vane assembly and several modifications were dentified in order to adapt the model to full-scale applications.

0 DISTRIBUTION / AVAILABILITY OF ABSTRACT	21 ABSTRACT SECURITY CLASSIFICATION
☒ UNCLASSIFIED/UNLIMITED ☐ SAME AS RPT ☐ DTIC USERS	UNCLASSIFIED
2a NAME OF RESPONSIBLE INDIVIDUAL Prof Nunn	22b TELEPHONE (Include Area Code) (408) 646-2365 22c OFFICE SYMBOL 69Nn

D FORM 1473, 84 MAR 83 APR edition may be used until exhausted
All other editions are obsolete

SECURITY CLASSIFICATION OF THIS PAGE

☆ U.S. Government Printing Office 1986—606-243

Approved for public release; distribution is unlimited.

Modeling Transient Thermal Behavior in a Thrust Vector Control Jet Vane

by

Margaret Mary Reno
Lieutenant, United States Navy
B.A., California State University at Long Beach, 1979

Submitted in partial fulfillment of the
requirements for the degree of

MASTER OF SCIENCE IN MECHANICAL ENGINEERING

from the

NAVAL POSTGRADUATE SCHOOL
December 1988

ABSTRACT

An attempt was made to model the transient thermal response of jet vanes used for thrust control. A simple computer model based on lumped capacitance methods using boundary layer convection and stagnation point heating as thermal inputs appeared to adequately predict temperatures for a quarter-scale model. This report details the attempt to enlarge the model to allow comparison between thermal predictions and the results of tests on a full-scale prototype jet vane. It was determined that the model could not be considered a thermal representation of the full-scale vane assembly and several modifications were identified in order to adapt the model to full-scale applications.

TABLE OF CONTENTS

LIST OF FIGURES

I. INTRODUCTION

Because of the need for maneuverability, the designs for tactical missiles and spacecraft launch vehicles require the application of active control systems. Thrust Vector Control (TVC) is one such system which gives the capability of trajectory control almost independent of the external forces of the vehicle. This independence is important when relative air flow past the vehicle's external lifting surfaces is too slow to generate the necessary control. Applications for TVC include low speed flight (during launch or while hovering, for instance) and some cases involving high angle of attack. Also, in cases where missiles are launched from tubes it is often impossible to provide adequate external control surfaces.

One method of TVC is the insertion of a jet vane into the exhaust of a rocket nozzle allowing vehicle control immediately after launch. This system, while allowing for large thrust deflection and rapid response, also results in thermal problems and some thrust loss. Calculation of the heat transfer characteristics is made difficult due to the severe thermal environment. So a reliable, dynamic computational model would be beneficial in assisting design efforts. Such a model of the thermal process in the jet vane is used in this report. This model was developed in support of a larger program at the Naval Weapons Center

(NWC), China Lake, CA, using data from a 1/4 scale retractable jet vane employed in the Stowable Three-Axis Reaction Steering (STARS) System, Figure 1.1. The purpose of this report is to verify the applicability of the results gained from 1/4 scale testing to full scale prototypes.

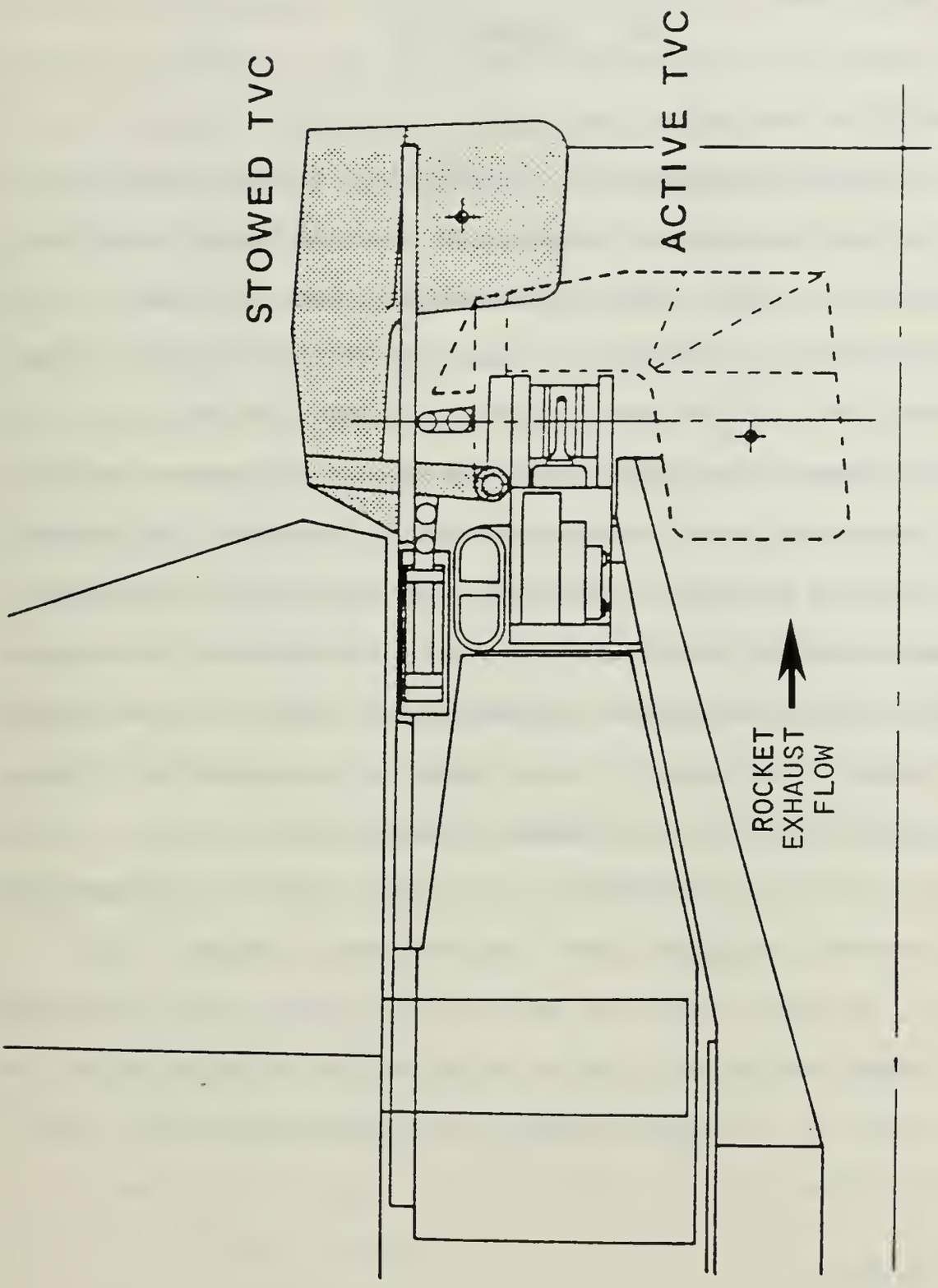

Figure 1.1. STARS TVC Stowage Concept

II. BACKGROUND

A. THEORY

The traditional approach to modeling a heat transfer system such as this is to construct a comprehensive model that treats the flow environment of the vane in fine numerical detail. However, a complete analysis would have to account for multi-phase, multi-component, three-dimensional and time dependent effects in the presence of shocks, boundary layer transition and turbulence, separated flows, surface ablation, chemical reaction and solid-body and gaseous radiation [Ref. 1]. Vast simplification can be achieved if the assumption is made that sufficient accuracy can be gained when the flow and vane are considered to be made up of relatively few thermal components and by realizing that the net effect of all the above complications is to transfer energy to and from the vane system. The transient thermal responses measured at accessible locations on the vane (protected from or outside the exhaust flow) can then be used to estimate temperatures achieved by the vane inside the flow.

B. THE MODEL

Work on the jet vane thermal model was begun at the Naval Postgraduate School (NPS) in 1986 by Nunn and Kelleher [Ref. 1]. Development of the model was continued by Nunn

[Ref. 2] and Hatzenbuehler [Ref. 3]. A result of these studies is a model, Figure 1.2, of the jet vane undergoing testing at NWC. The important features of this model are that it can be described using four nodes and applying lumped capacitance procedures. The purpose of node 1, the vane tip, is to account for stagnation properties of thermal convection near the vane leading edge. The fin is the remaining portion of the vane exposed to the rocket exhaust-gas temperatures, and is modeled by node 2. This node is subject to heat transfer by both turbulent convection and conduction. Node 3 is the vane shaft with heat transfer assumed to take place by conduction only and node 4 represents the mount connecting the shaft to the rocket frame, also subject to conduction only. Details of the model are contained in Reference 2, pages 9-11, and Reference 3. The governing equations for heat transfer in this model, become [Ref, 2, p.31, Ref 3]:

$$\dot{T}_1 = -(T_1/C_1)(1/R_{F1} + 1/R_{12}) + T_2(1/C_1R_{12}) + T_{R1}(1/C_1R_{F1}) \quad (1)$$

$$\dot{T}_2 = (T_1/C_2)(1/R_{12}) - (T_2/C_2)(1/R_{F2} + 1/R_{12} + 1/R_{23}) + (T_3/C_2)(1/R_{23}) + (T_{R2}/C_2)(1/R_{F2}) \quad (2)$$

$$\dot{T}_3 = (T_2/C_3)(1/R_{23}) - (T_3/C_3)(1/R_{23} + 1/R_{34}) + (T_4/C_3)(1/R_{34}) \quad (3)$$

$$\dot{T}_4 = (T_3/C_4)(1/R_{34}) - (T_4/C_4)(1/R_{34}+1/R_{4G}). \quad (4)$$

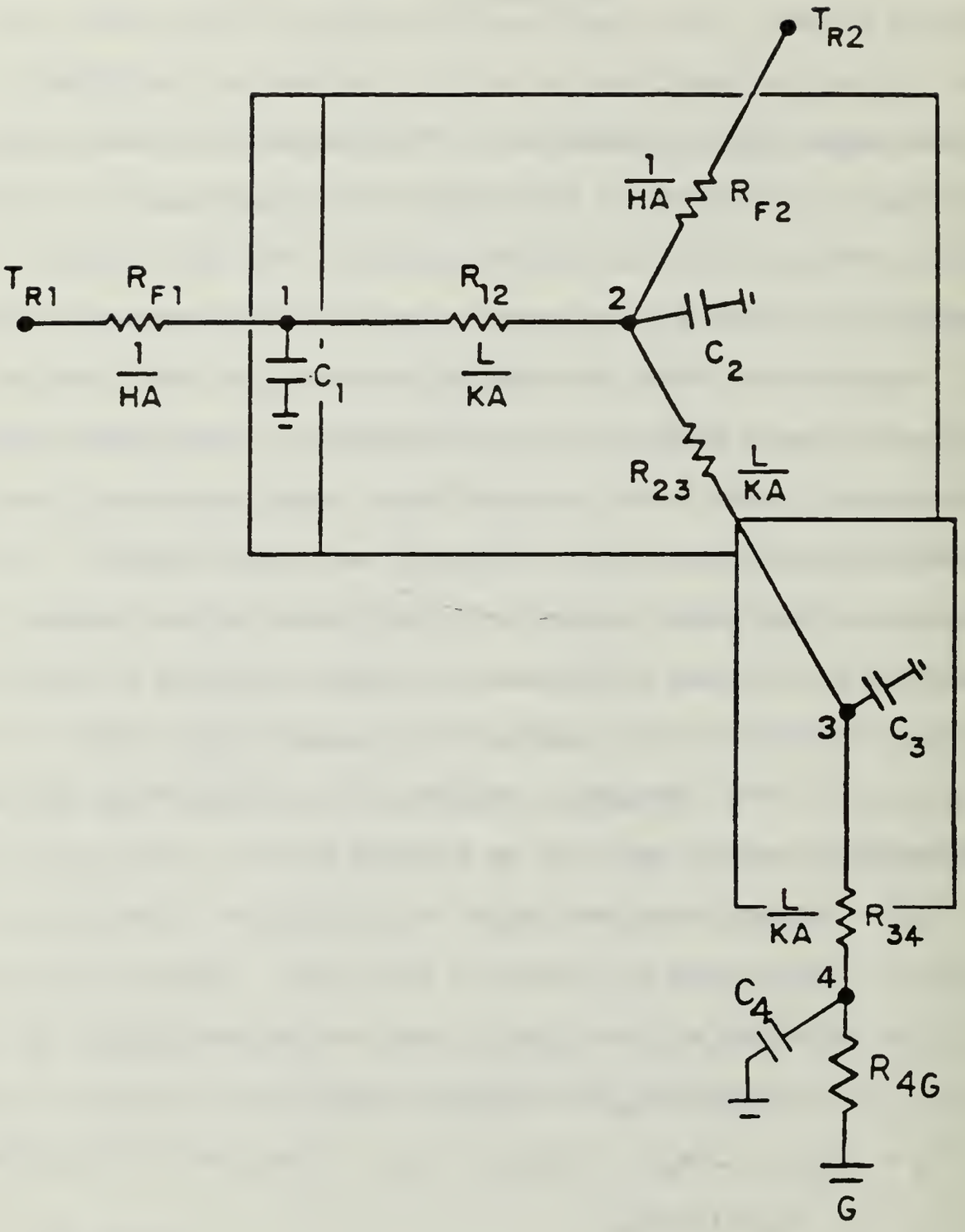

Figure 1.2. Four Node Model Configuration

Here, the subscript R refers to recovery temperatures which are used because, due to the high speed in the compressible boundary layer, the temperature driving the heat transfer will exceed the local static temperature of the exhaust. It should be noted that each of the temperature coefficients on the right-hand sides of Eqs. (1)-(4) have the dimensions of inverse time. In fact, the RC products are representations of the time constants describing the energy transport processes occurring at and around the nodes. Among the several resistances and capacitances appearing in the model, those believed to be most uncertain in their values are the input resistances due to convection, and the time constants associated with conduction through the mount.

System identification procedures were used to determine what these values should be in order to provide agreement with temperature histories recorded for the shaft and mount during NWC test firings on the 1/4 scale vanes. The initial values used for resistance and capacitance are listed in Appendix A.

C. SYSTEM BUILD

It was decided to construct the simulation model using a personal computer (PC) version of System Build and System Identification developed by Integrated Systems, Inc. [Ref. 4, 5]. In order to simplify the code, the following parameters were defined for use in Eqs. (1)-(4):

$a_{11} = (a_{12}+b_{11})$ $a_{12} = 1/C_1R_{12}$

$a_{21} = 1/C_2R_{12}$ $a_{22} = a_{21} + a_{23} + b_{22}$ $a_{23} = 1/C_2R_{23}$

$a_{32} = 1/C_3R_{23}$ $a_{33} = (a_{32} + a_{34})$ $a_{34} = 1/C_3R_{34}$

$a_{43} = 1/C_4R_{34}$ $a_{44} = a_{43} + a_{4G}$ $a_{4G} = 1/C_4R_{4G}$

$b_{11} = 1/C_1R_{F1}$ $b_{22} = 1/C_2R_{F2}$

These are referred to as the characteristic rates of the model, and the resulting equations for input to system build become:

$$\dot{T}_1 = -a_{11}T_1 + a_{12}T_2 + b_{11}T_{R1} \quad (5)$$

$$\dot{T}_2 = a_{21}T_1 - a_{22}T_2 + a_{23}T_3 + b_{22}T_{R2} \quad (6)$$

$$\dot{T}_3 = a_{32}T_2 - a_{33}T_3 + a_{34}T_4 \quad (7)$$

$$\dot{T}_4 = a_{43}T_3 - a_{44}T_4 \quad (8)$$

The System Build thermal model consists of nine Super Blocks:

NOD1IN, NOD2IN, NOD3IN, NOD4IN,

NODE1, NODE2, NODE3, NODE4,

VANE,

as shown in Appendix B. The input is a ramp-up, plateau, ramp-down to provide for the transient stagnation temperature profile generated by the rocket motor firing, [Ref. 2, p.23]. The first four blocks compute the parameters necessary for the equations. The ramp-up, plateau, ramp-down input to NOD1IN and NOD2IN has a maximum value of unity. In NOD1IN, for example, this input is multiplied by

b_{11} and T_{R1} as gains to form the time varying element in eq.(5). Also, in NOD1IN, a_{12} is generated by a step function and added to b_{11} to form a_{11}. So the outputs of NOD1IN are a_{11}, $b_{11}T_{R1}$ and a_{12}.

In NODE1 the outputs of NOD1IN are combined with the external input, T_2, to form eq.(5). The integrator then converts $\dot{T}_1$ to T_1 which is the NODE1 output. NODE2, NODE3 and NODE4 are similar in form and function and generate T_2, T_3 and T_4 respectively. The super block, VANE, interconnects these last four blocks and provides the simultaneous solution for the four nodal temperatures. The step amplitude and gain parameters in any of the blocks may be varied to facilitate system identification. When a parameter is allowed to vary, System ID will calculate the value which allows the closest fit of the model predictions to actual test data curves.

This simulation was run initially with only a 3-node model using the mount as ground for reference [Ref. 2] and setting the mount thermal resistance as an adjustable parameter. Because of a fault in connecting the System Build super blocks, erroneous results were obtained for the values of b_{22} and a_{33} [Ref. 2, p. 45]. After removing the fault, the following corrected values were obtained: $b_{22} = 0.1956\ s^{-1}$ and $a_{33} = -0.4827\ s^{-1}$. These values were obtained through System Identification using the NWC transfer function for T_3 [Ref 2, P. 24] for comparison with the simulation results.

III. APPROACH

A. STARTING POINT

The coefficient values obtained by Hatzenbuehler [Ref. 3] were also based on faulty System Build model, and these numbers were re-calculated before attempting to scale up the model. Using event 2 data from Reference 3 [Appendix C], the model was again set up for system identification with the MAXLIKE function of MATRIXx [Ref 5]. Four parameters were allowed to vary simultaneously and were compared to test data temperatures recorded from the shaft (Node 3), and the mount (Node 4). Initial values for all parameters are contained in Appendix D. The parameters which a were allowed to vary were:

- b_{22} - allows estimation of the value of R_{F2}, the resistance to heat transfer to the fin surface,
- a_{34} - allows estimation of R_{34}, the resistance to conduction through the shaft,
- a_{43} - given a_{34}, allows estimation of the capacitance of the mount, C_4, and
- a_{4G} - allows an estimate of the conductive resistance to heat transfer through the mount to the environment, R_{4G}.

Three (3) iterations of MAXLIKE returned the values of:

$$b_{22} = 0.2718\ s^{-1},\ a_{34} = 0.299\ s^{-1},\ a_{43} = 0.1322\ s^{-1}$$

and

$$a_{4G} = 0.1018\ s^{-1}.$$

These correspond to values of:

R_{F2} = 1.67 K/W, R_{34} = 3.33K/W,

C_4 = 2.27 J/K and R_{4G} = 4.33 K/W.

Figure 3.1 shows the excellent fit these values give to the test data. It should be noted that because of these new maximum-likelihood parameter values, the simulation results shown here are slightly different from those reported in Reference 3. For instance, the maximum vane tip temperature predicted for event 2 is 1438 K (1144 K above ambient), some 175 K higher than that reported in Reference 3.

B. ENLARGING TO FULL SCALE

In the time since this study began, NWC China Lake has begun testing of full-scale prototype jet vanes. With the larger vane it became possible to insert thermocouples inside the fin in locations corresponding to some of the nodes in the thermal model. The only node still inaccessible for actual measurement was the vane tip, where the highest temperatures were expected to occur. Therefore, an attempt was made to "scale up" the computer thermal model to compare with the results of the prototype testing.

Three important differences between the sub-scale and full scale testing configurations must be noted. In the 1/4-scale testing, four fixed vanes were arranged symmetrically in the jet nozzle. Only three vanes were used in the full-scale firing and one of these was deflected

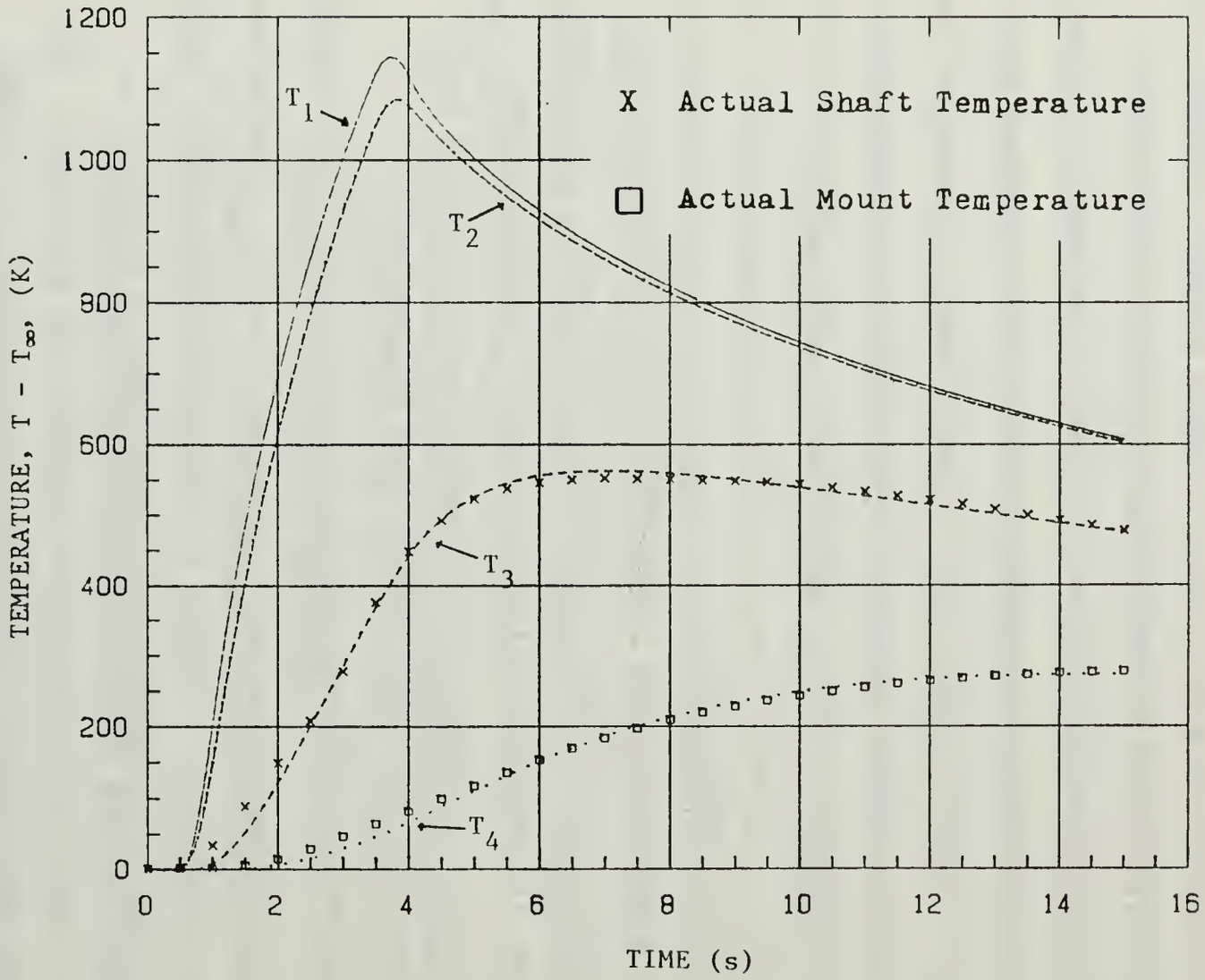

Figure 3.1. Temperature Histories, Four Node Model

intermittently during the test. Though these vanes were also arranged symmetrically, it is likely that the heat-transfer rates were significantly affected by the different shock-wave patterns generated through the vane arrangement. Additionally, although the full-scale vanes were assumed to have been strictly proportional to the sub-scale model, the mounting apparatus was not. In fact, no consistent mount arrangement was used during the 1/4-scale testing [Ref 3]. Since consistent data for the resistance to heat transfer in the mount, and from there to ground, was unavailable, it was decided to return to the 3-node thermal model [Ref 2] which connects the shaft node directly to ground. This model is summarized in Appendix E. Without geometric similarity between the two mounting configurations there was little reason to believe that the time constants relating to the mount could be scaled directly. Finally, in video recordings [Ref. 6] of the full-scale tests, both the vane mounts and the jet nozzle wall exhibited indications of more rapid heating than in the subscale tests. The prototype mounting apparatus included fin-like extensions parallel to the flow and subject to convective heat transfer. Also, the nozzle wall was proportionally much thinner in the full-scale firings. This would have allowed the nozzle to reach higher temperatures. As will be discussed, this work has shown that these effects may have significantly altered the

radiation environment of the jet vanes resulting in faster heat-up transients and a longer cool-down period following motor burnout.

For the characteristic coefficients affecting only the vane and shaft nodes, it was felt that direct scaling was appropriate. The characteristic rate, a_{12}, in the 1/4 scale model, for example, is decreased to its full-scale value by the following method:

$a_{12} = 1/C_1R_{12}$

$C = \rho\ c_pV$

$R = L/k\ A$

ρ - density

c_p - specific heat

V - volume

L - Length

k - thermal conductivity

A - area

Let the subscript f denote full scale values and s the values corresponding to reduced scale. Then knowing that the thermal diffusivity, $\alpha=k/\rho c_p$, remains constant during scaling:

$$a_{12s} = \alpha A_s/(V_s\ L_s)$$
$$= \alpha\ A_f\ (\text{scale})^2/[V_f\ (\text{scale})^3\ L_f\ (\text{scale})]$$
$$= a_{12f}/(\text{scale})^2$$

or

$$a_{12f} = a_{12s}\ (\text{scale})^2.$$

In this case (scale) is 1/4 and $a_{12s}=4.7\ s^{-1}$, so

$$a_{12F} = (4.7)(1/4)^2 = 0.294\ s^{-1}.$$

The remainder of the characteristic rates governing conduction in the model were similarly scaled.

The characteristic rates governing convection were scaled according to the procedure outlined in Reference 2 (p.20). Stagnation point thermal resistance decreases as $(0.25)^{-1.5}$. However, upon review of the equations, it was determined that boundary layer thermal resistance should be proportional to $(0.25)^{-1.8}$. For instance, the stagnation point characteristic rate is given by:

$$b_{11s} = 0.45\ s^{-1}$$
$$= 1/[C_f\ (0.25)^3 R_{1f}\ (0.25)^{-1.5}]$$
$$= 1/C_f R_{1f} (0.25)^{-1.5}$$
$$= b_{11f}/(0.25)^{1.5}$$

and,

$$b_{11f} = (0.25)^{1.5}(b_{11s}) = 0.0563\ s^{-1}.$$

The entire set of coefficient values for the full-scale thermal model is given in Appendix F.

C. SIMULATION

Additional information required before the computer model can be executed includes the recovery temperatures and the input function modeling the thrust. From evaluation of the propellant properties, NWC, China Lake calculated the stagnation temperature as being 2971 K. Ambient temperature was not reported but, based on the initial readings of the 21 thermocouples used, and accounting for their differences

according to their location, T_{AMB} was chosen as 301 K. T_{R2} was then calculated using the procedures of Reference 2 (pp. 17-21). Referring the recovery temperatures to ambient yields T_{R1} = 2670 K and T_{R2} = 2567 K. These are the values used in the model.

The thermal input schedule was modified to synchronize with the thrust trace obtained from the full scale firing as shown in Figure 3.2 The resulting normalized thrust function, for input to super-blocks NOD1IN and NOD2IN of the model is given in Table I.

As can be seen from Figure 3.3, simulation with the model under the assumption of full thermal scaling failed to predict the temperature of node 2, much less to give a reasonable estimate for the temperature of node 1, the node of interest. This leads to the conclusion that the differences between the two (large and small) devices are not adequately described by a single scale factor. However, investigation proceeded to determine if the model could, in fact, still serve the purpose for which it was constructed: to predict the maximum temperatures at the vane tip and other locations of special interest.

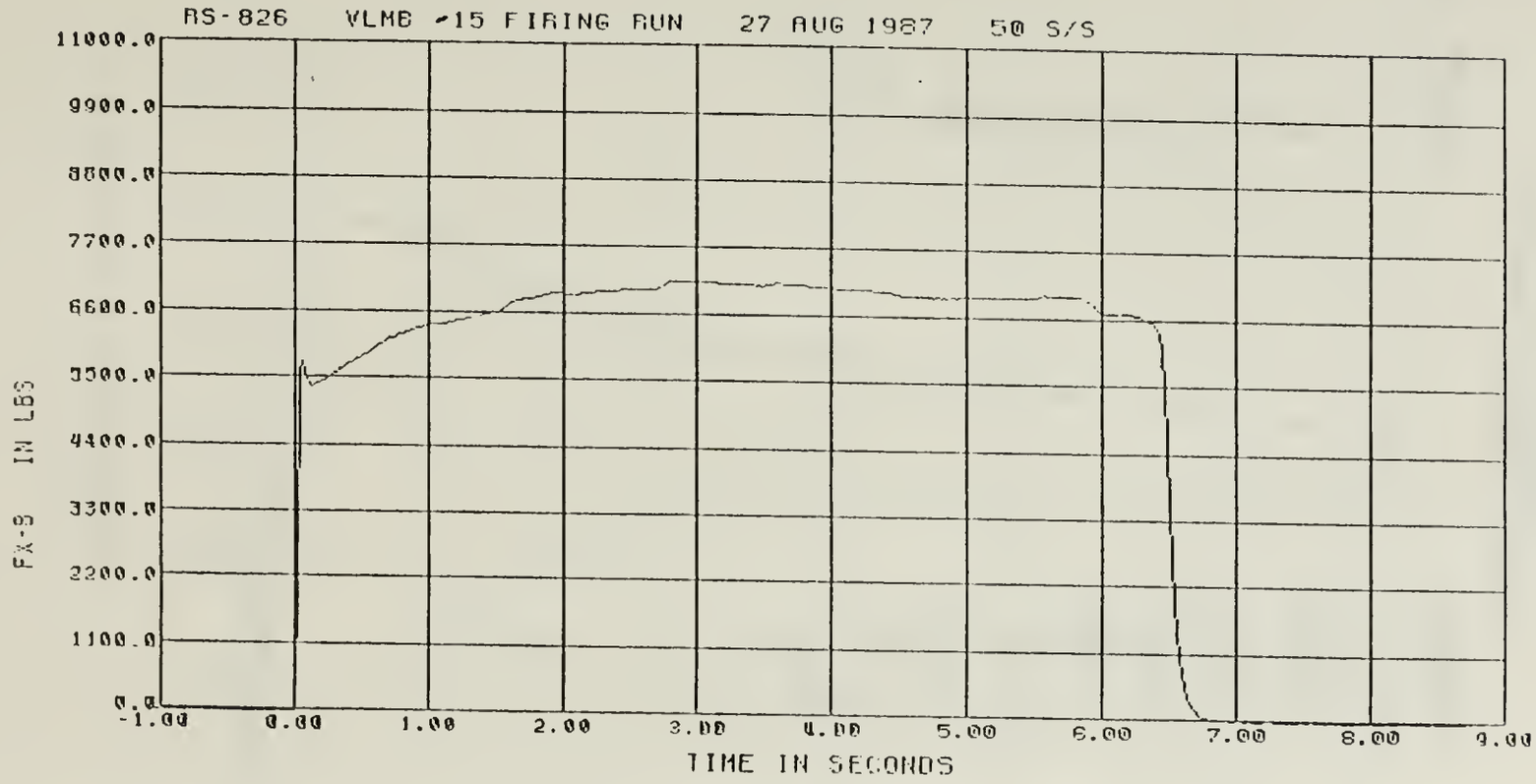

Figure 3.2. NWC Thrust Trace, Prototype Testing

TABLE I.
Input Thrust Function

TIME(S)	THRUST (%)
0	0
0.07	81
0.14	78
1.67	100
5.81	100
6.0	94
6.35	94
6.70	0
120.0	0

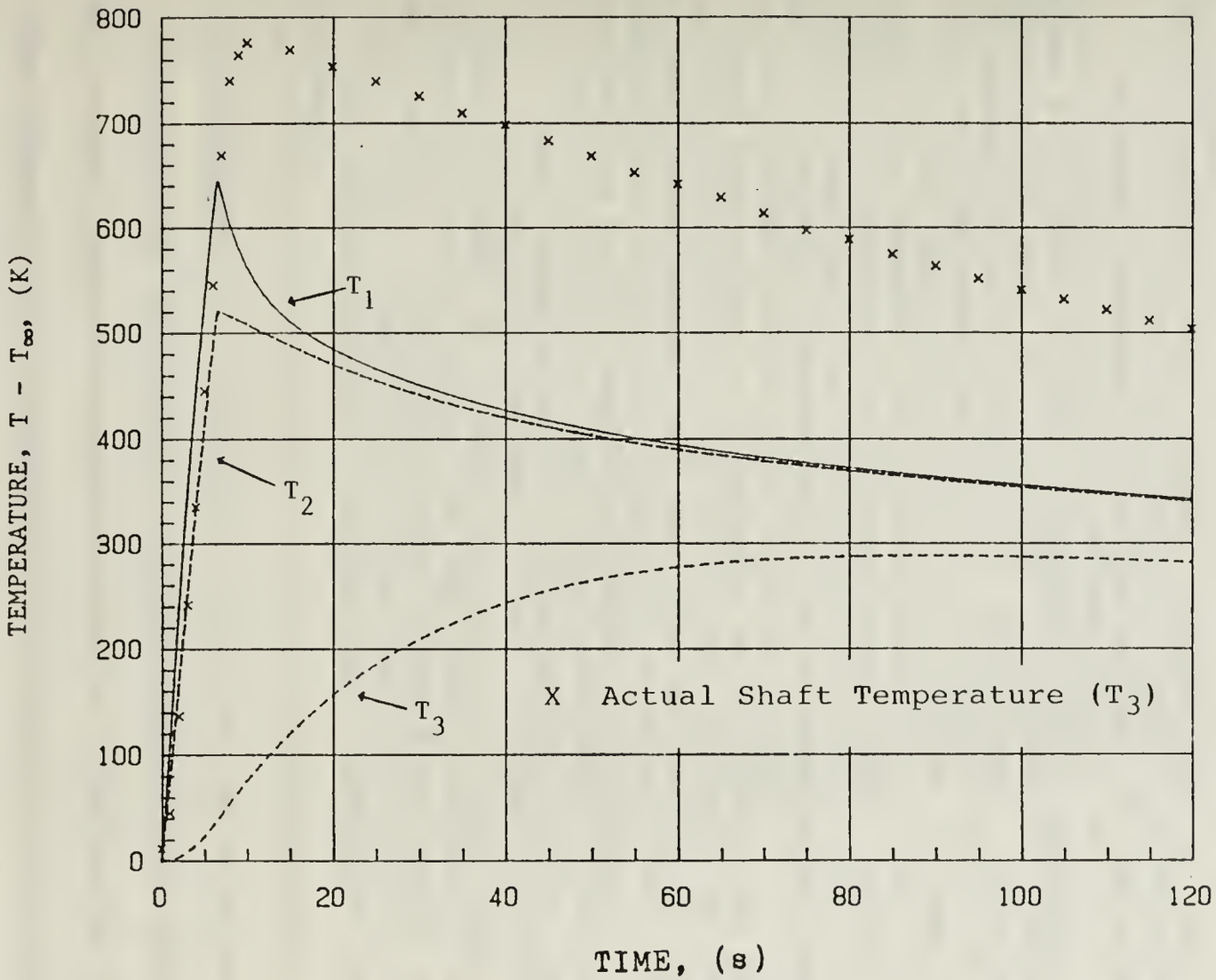

Figure 3.3. Temperature Histories Based on Conventional Scaling Procedures

IV. REVISED PROCEDURE

A. EXAMINATION

In order to gain further insights from the model it was first necessary to realize where the probable inconsistencies occurred in the assumption that it could be a scaled representation. One source of possible error is related to the fact that in modeling the subscale process [Ref 2, 3] the net thermal input resistances were increased to values well above those based solely upon thermal convection. Such increases were found to be necessary to obtain good agreement with the 1/4-scale data, but the present model does not provide a rationale for adjusting these factors on the basis of scale. Such a rationale would have to come from a thermal model that includes the effects of radiation and ablation on the net thermal input resistance. Further, as previously mentioned, the radiation effects in the two testing configurations appeared to be drastically different.

In addition to the input resistance, the thermal heat sink effect of the mount (output resistance) was also not amenable to scaling. Since variations of these factors can have significant impact on the agreement of the model with known data, it was decided to apply System Identification with the known shaft temperature of the full scale prototype to see if matching this temperature would successfully predict the temperatures at nodes elsewhere on the test

vanes. Once again parameters a_{33} and b_{22} were allowed to vary. Full scale values [Appendix F] of the other parameters were used.

B. RESULTS

Figure 4.1 shows the lack of success with this approach. While allowing the modeled temperatures at node 3 to approach the data for the shaft, the remaining temperatures increased disproportionately, to the point where the node 2 temperature reached its maximum value, T_{R2}. What became apparent was that the temperature profiles of the data for the full scale testing were quite different from those for the subscale test firings. The rapid increase in the data temperatures in the first ten seconds more closely followed the expected rise for those nodes receiving direct thermal input from the surroundings. Thus, it became apparent that in the full-scale tests, the shaft was receiving significant thermal input in addition to that due to conduction through the vane.

C. CONCLUSION

Because of the change in testing conditions the 1/4-scale model cannot be used directly to predict the required temperatures. Some source of direct heat input to the shaft (e.g., via radiation) seems to be indicated. Without this direct heat input, any attempt to match the data temperature

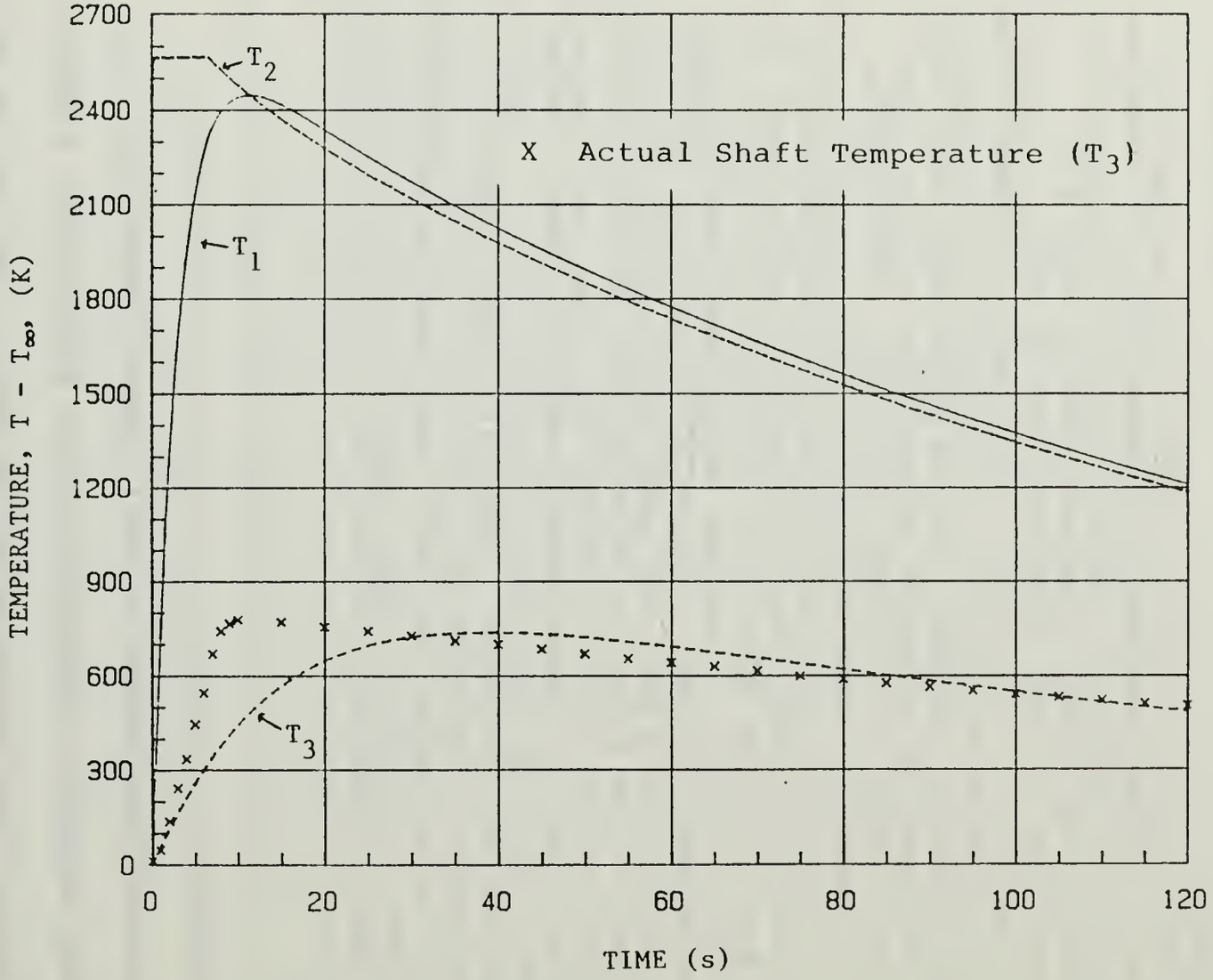

Figure 4.1. Temperature Histories After SYSTEM ID

for the shaft to the model's predictions causes vast distortion of predicted temperatures elsewhere on the vane. The two test configurations--"large" and "small"--were not scale models of each other from a heat transfer point of view.

APPENDIX A
[Reference 2]
Resistances and capacitances for 1/4-scale model

$$R_{F1} = 20.3 \text{ K/W}$$

$$R_{F2} = 2.3 \text{ K/W}$$

$$*R_{23} = 2.1 \text{ K/W}$$

$$C_1 = 0.11 \text{ J/K}$$

$$C_2 = 2.2 \text{ J/K}$$

$$C_3 = 1.0 \text{ J/K}$$

$*R_{23}$ is revised to agree with the corrected 3-node model

APPENDIX B

System Build Blocks For 4 Node Model

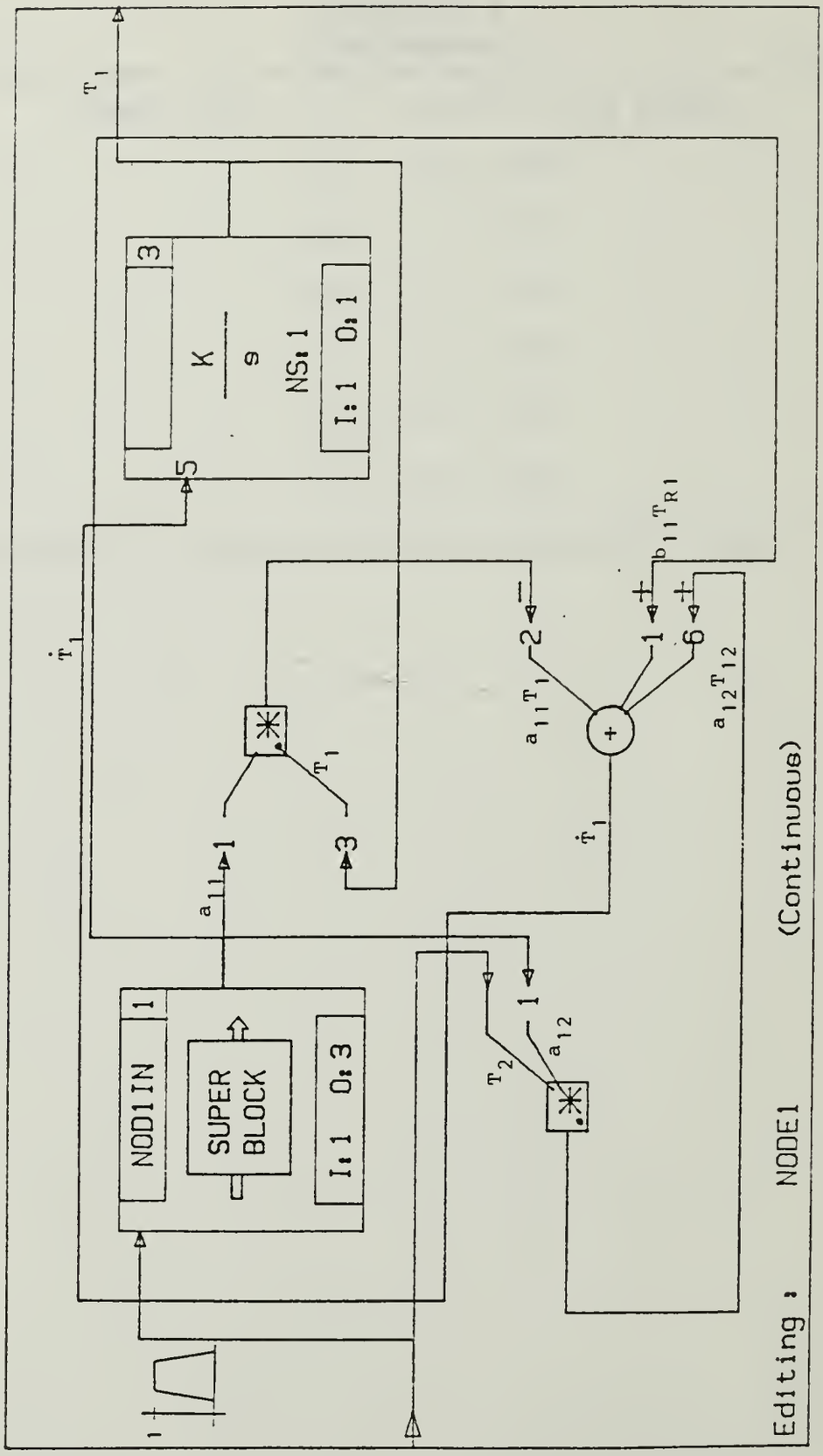
NOD1 IN
SUPER BLOCK
I: 1 O: 3
K
s
NS: 1
I: 1 O: 1
Editing : NODE1 (Continuous)

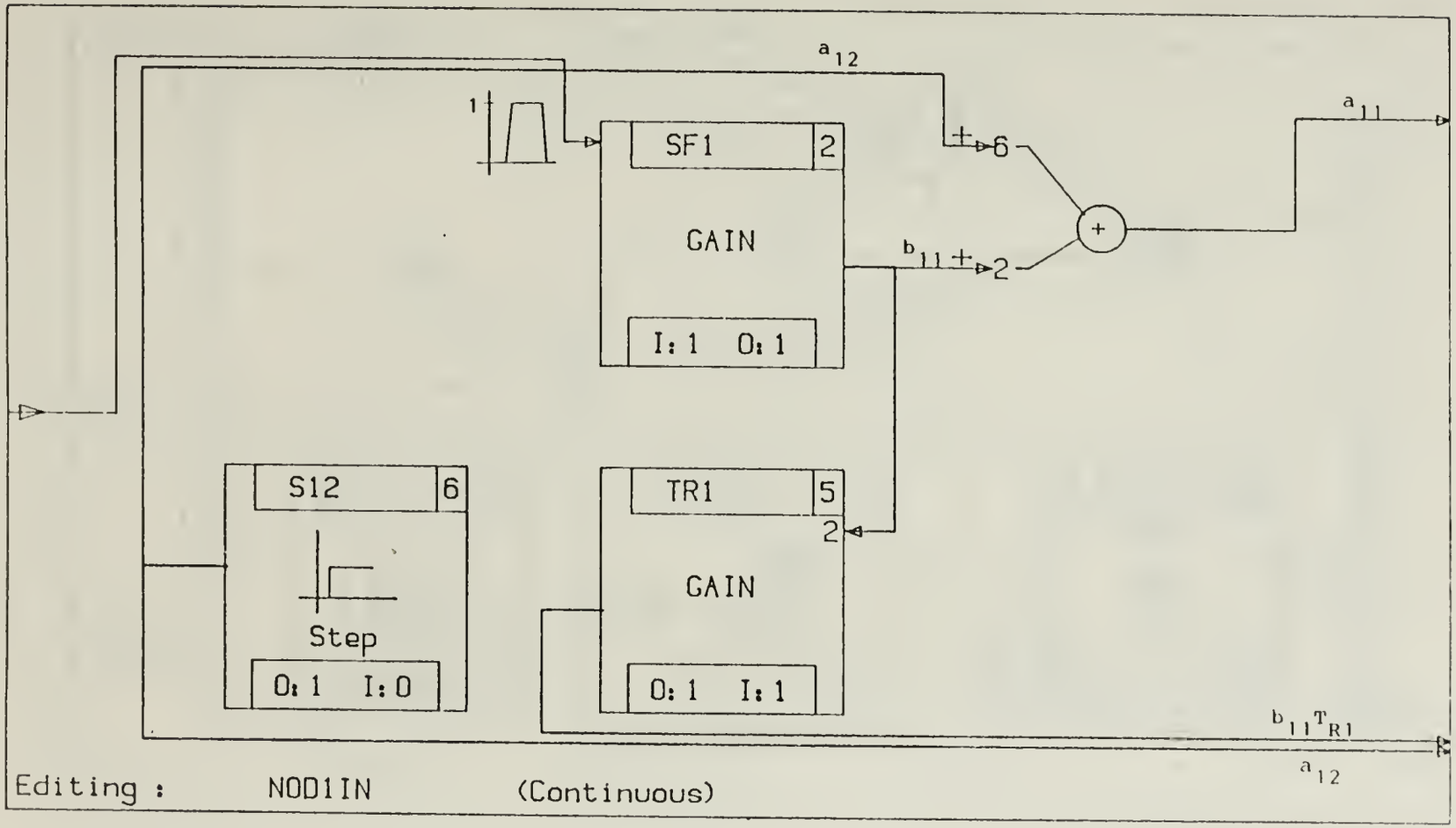
a12
1
SF1
2
GAIN
I: 1 O: 1
+
6
b11 +
2
a11
S12
6
Step
O: 1 I: 0
TR1
5
2
GAIN
O: 1 I: 1
b11TR1
a12
Editing : NOD1IN (Continuous)

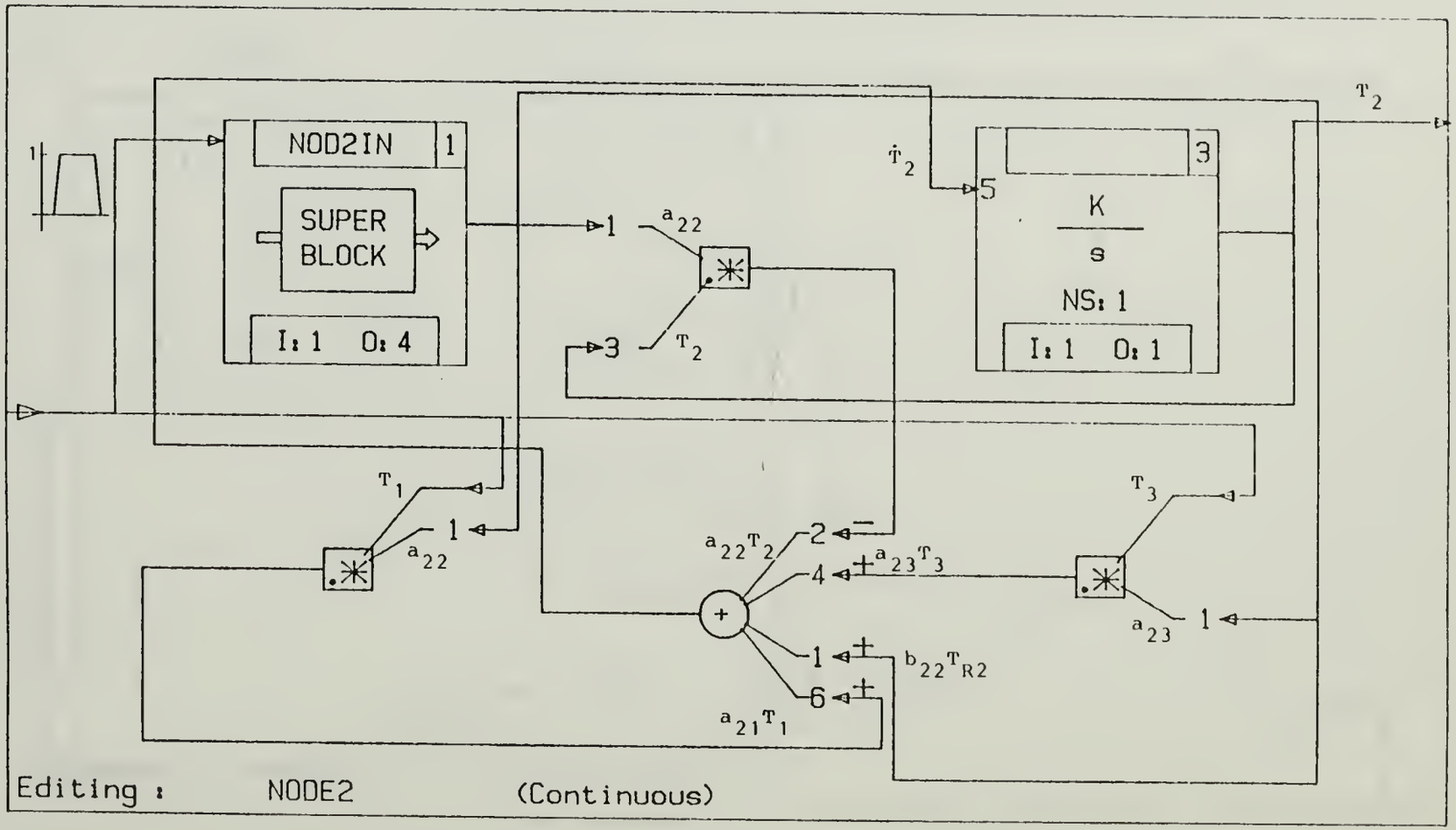
NOD2IN
1
SUPER
BLOCK
I: 1 O: 4
1
a22
3
T2
Ṫ2
5
3
K
s
NS: 1
I: 1 O: 1
T2
T1
1
a22
2
a22T2
4
a23T3
T3
a23
1
1
b22TR2
6
a21T1
Editing : NODE2 (Continuous)

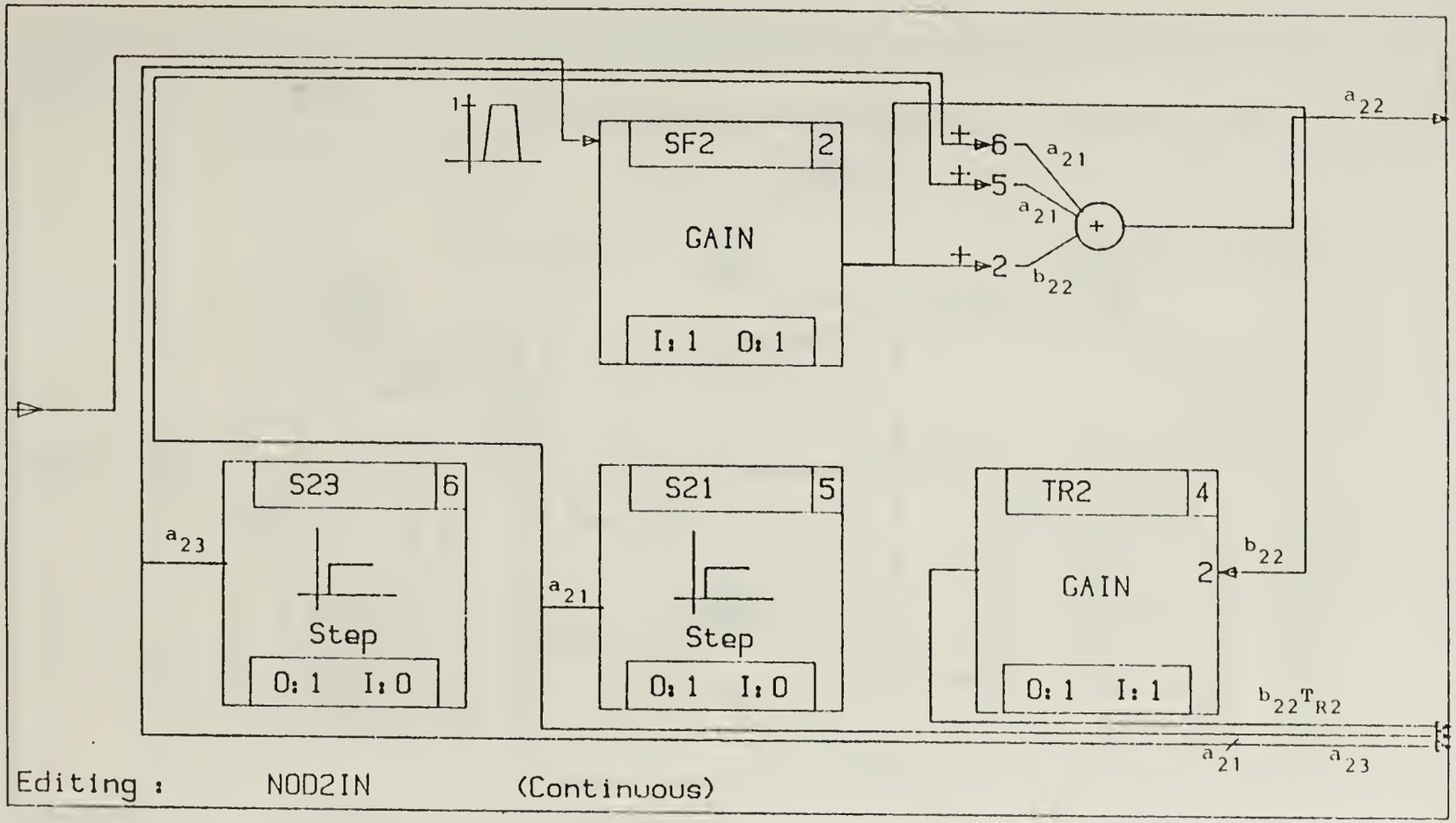
SF2
2
GAIN
I: 1 O: 1
1
6
5
2
a21
a21
b22
a22
S23
6
a23
Step
O: 1 I: 0
S21
5
a21
Step
O: 1 I: 0
TR2
4
GAIN
2
b22
O: 1 I: 1
b22TR2
a21
a23
Editing : NOD2IN (Continuous)

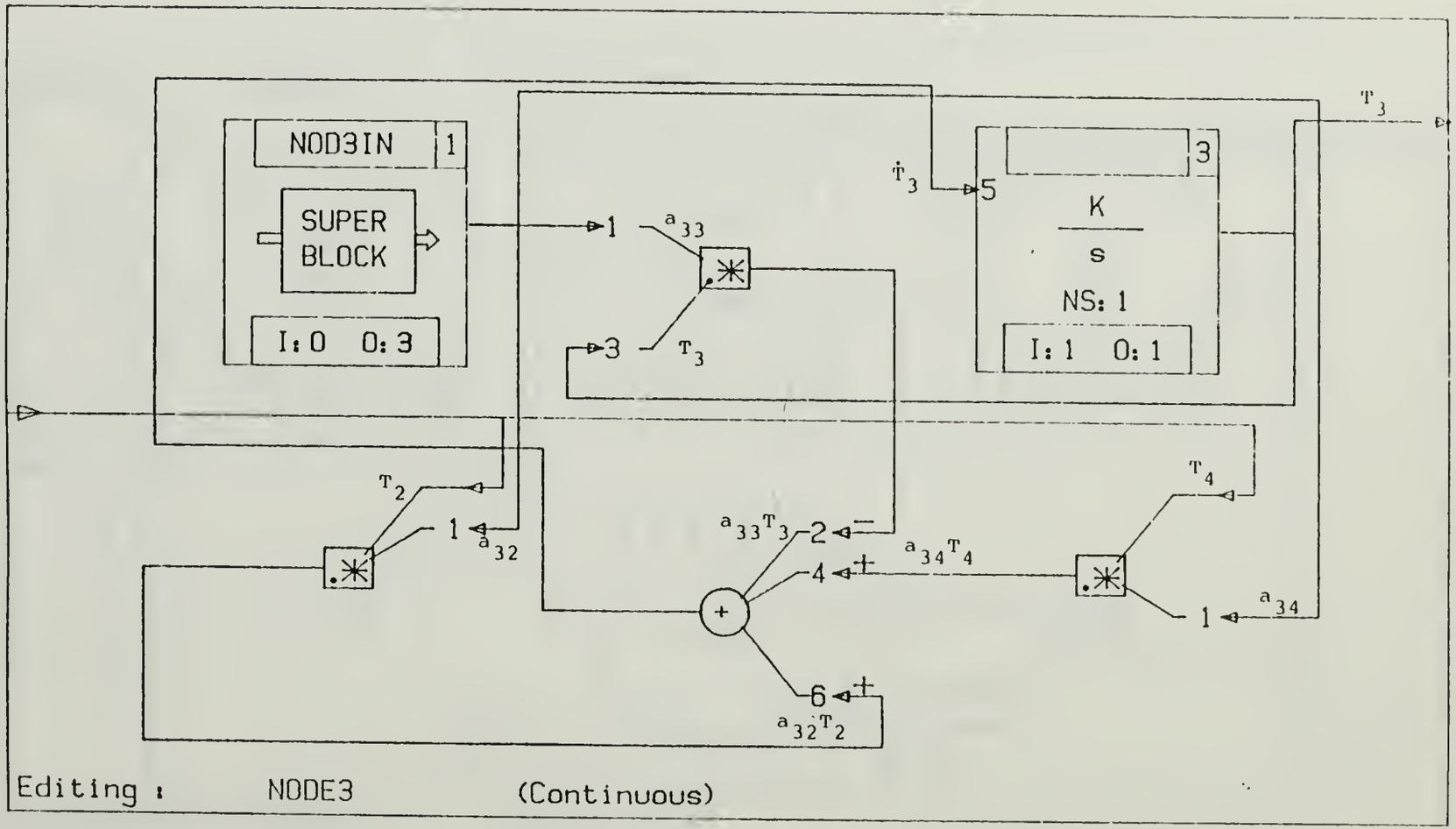
NOD3IN
1
SUPER
BLOCK
I: 0 0: 3
1
3
a_{33}
T_3
$\dot{T}_3$
5
3
K
s
NS: 1
I: 1 0: 1
T_3
T_2
1
a_{32}
$a_{33}T_3$
2
4
$a_{34}T_4$
T_4
1
a_{34}
6
$a_{32}T_2$
Editing : NODE3 (Continuous)

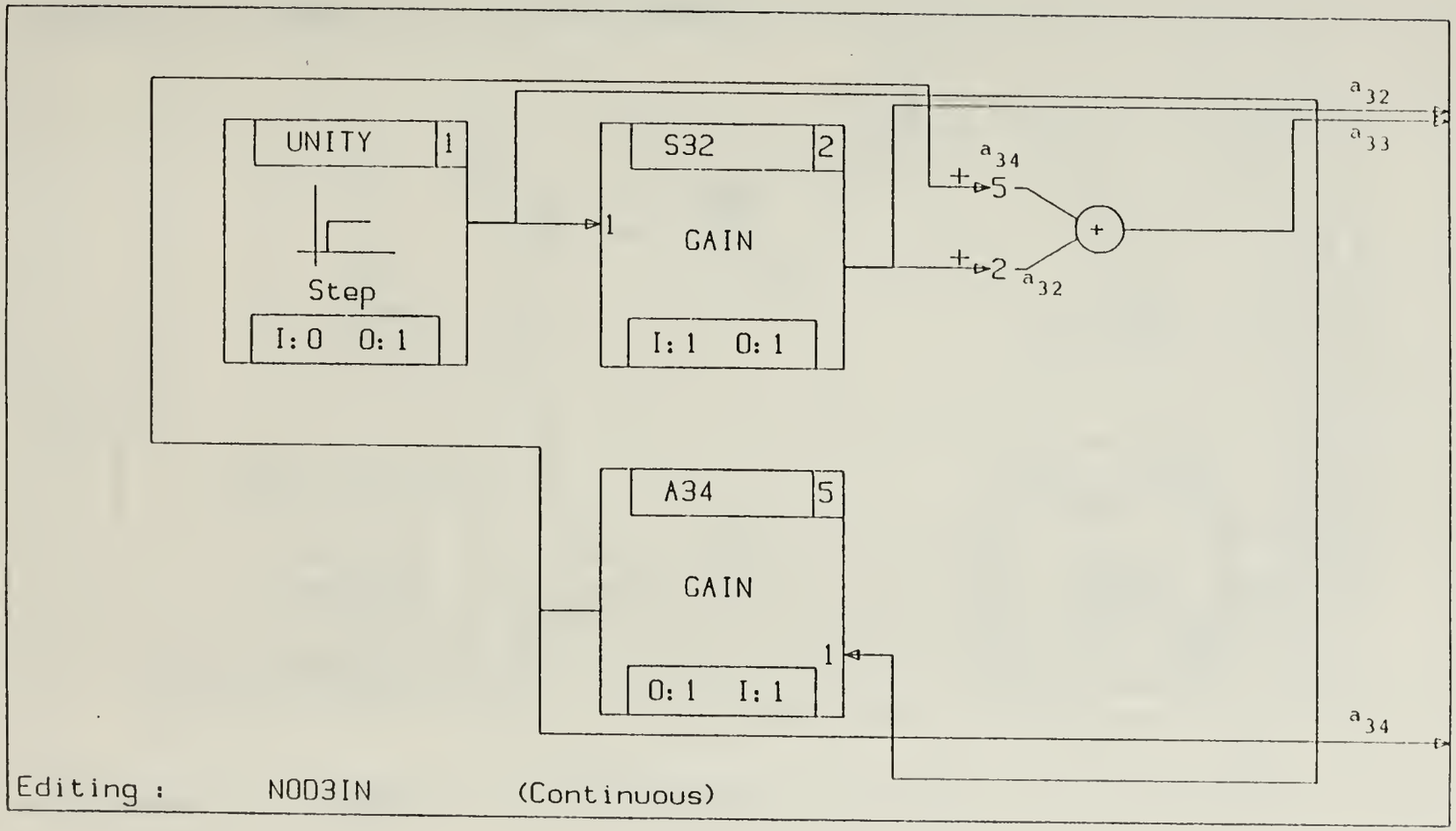
UNITY
1
Step
I: 0 O: 1
S32
2
GAIN
I: 1 O: 1
1
a34
+
5
+
2
a32
+
a32
a33
A34
5
GAIN
1
O: 1 I: 1
a34
Editing : NOD3IN (Continuous)

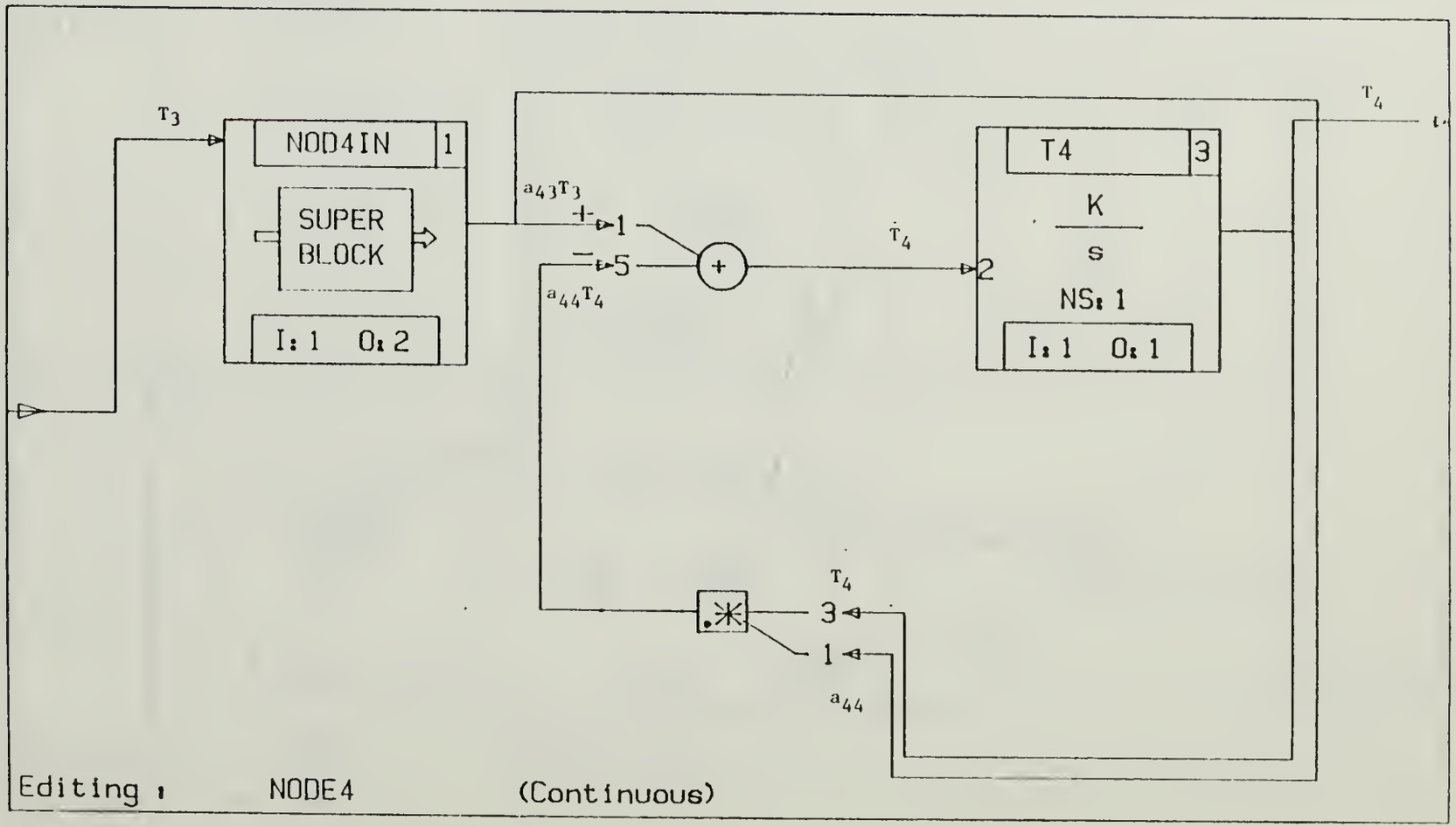
T3
NOD4IN
1
SUPER
BLOCK
I: 1 O: 2
a43T3
1
5
a44T4
+
T4
T4
3
K
s
NS: 1
I: 1 O: 1
2
T4
t
T4
3
1
a44
Editing : NODE4 (Continuous)

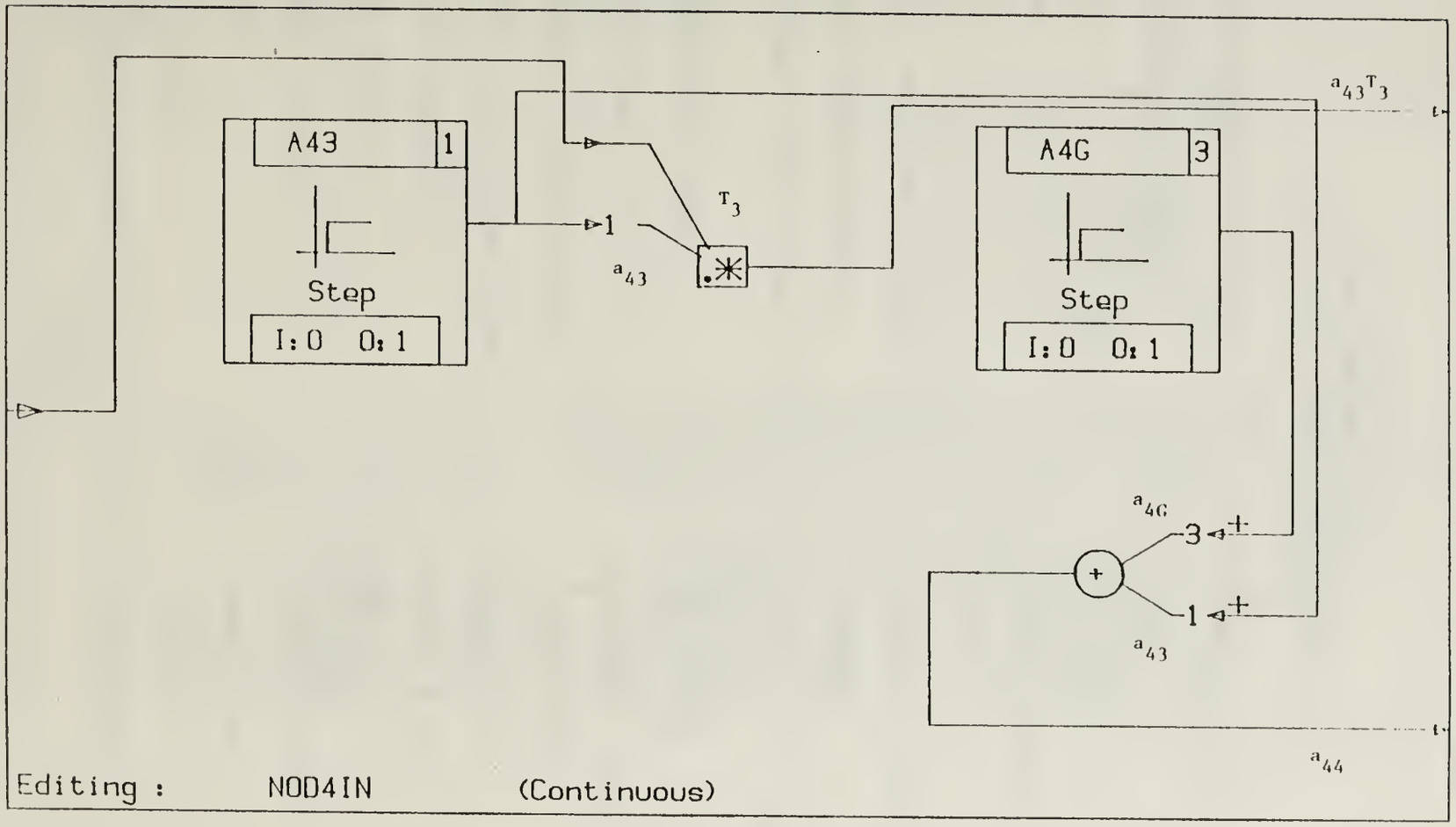
A43
1
Step
I:0 O:1
1
a_{43}
T_3
$a_{43}T_3$
A4G
3
Step
I:0 O:1
a_{4G}
3
+
1
a_{43}
a_{44}
Editing : NOD4IN (Continuous)

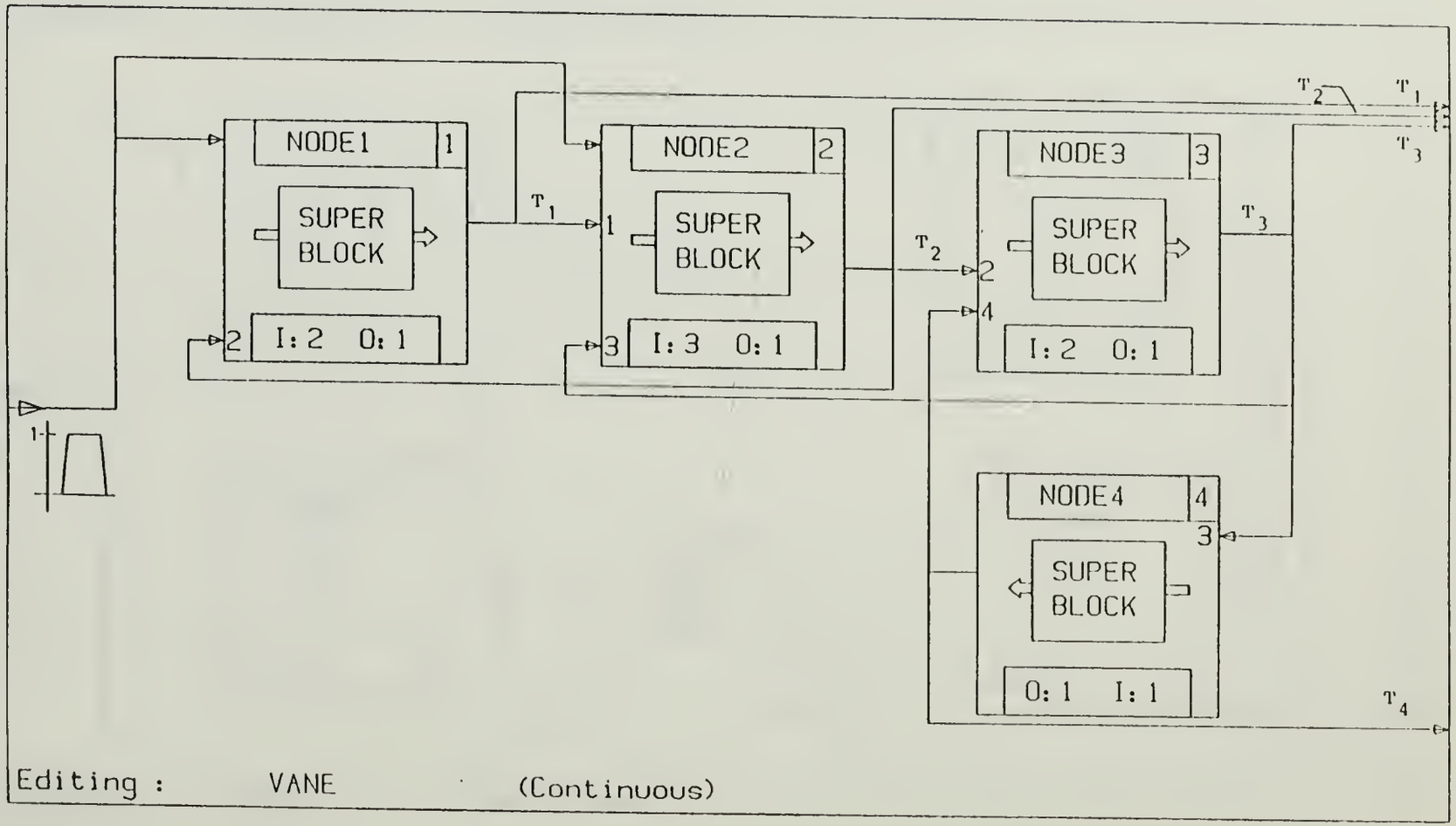
NODE1
1
SUPER
BLOCK
2
I: 2 O: 1
NODE2
2
SUPER
BLOCK
1
3
I: 3 O: 1
NODE3
3
SUPER
BLOCK
2
4
I: 2 O: 1
NODE4
4
3
SUPER
BLOCK
O: 1 I: 1
T1
T2
T3
T4
Editing : VANE (Continuous)

APPENDIX C
[Reference 3 APP.C]
NWC Test Firing Parameters

Propellant	0% AL HTPB
Molecular Weight	26.1
K=	1.210
C*=	4930 ft/sec
C_d=	0.934
Burn rate Coefficient =	.05703 in/sec
Burn rate exponent =	.28063
Ambient Conditions =	70 F, 13.7 PSIA
Propellant Mass =	6.17 lbm
Propellant Density =	.06185 lbm/in^3
Initial Throat Area =	.14750 in^2
Post-fire Throat Area =	.15135 in^2
Max Pressure =	2286.8 PSI
Max Thrust =	514 lbf
Total Impulse =	1535 lb-sec
ISP =	248.8 sec
Exit Dia =	1.8125"
Max Exit Pressure =	12.3 PSI

APPENDIX D
Initial Values For 1/4 Scale Model

NOD1IN

A12 = 4.7 s^{-1}

B11 = 0.45 s^{-1}

TR1 = 2360 K

NOD2IN

A21 = 0.23 s^{-1}

A23 = 0.18 s^{-1}

*B22 = 0.1956 s^{-1}

TR2 = 2260 K

NOD3IN

A32 = 0.38

*A34 = 0.17

NOD4IN

*A43 = 0.17

*A4G = 0.14

*parameter allowed to vary for SYSTEM ID

APPENDIX E
[Reference 2]
Three Node Heat Transfer Model

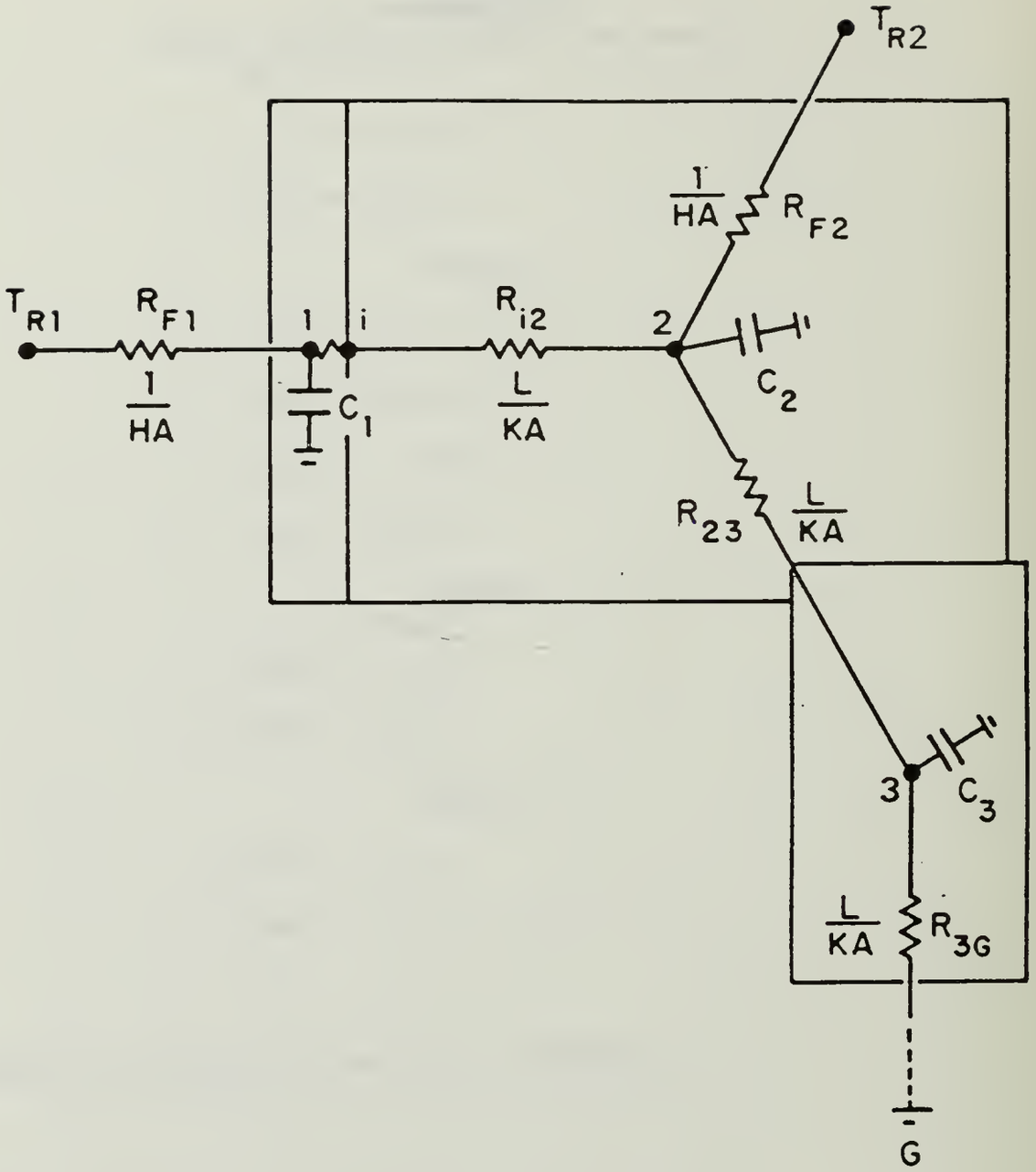

Figure E.1. Basic Three Node Model

Governing equations

$$\dot{T}_1 = -(T_1/C_1)(1/R_{F1} + 1/R_{12}) + (T_2/C_2)(1/R_{12}) + T_{R1}/C_1R_{F1}$$

$$\dot{T}_2 = (T_1/C_2)(1/R_{12}) - (T_2/C_2)(1/R_{F2} + 1/R_{12} + 1/R_{23}) + T_3/C_2R_{23} + (T_{R2}/C_2)(1/R_{F2})$$

$$\dot{T}_3 = (T_2/C_3)(1/R_{23}) - (T_3/C_3)(1/R_{23} + 1/R_{3G})$$

Characteristic Rates:

$$a_{11} = a_{12} + b_{11}$$

$$a_{12} = 1/C_1R_{12}$$

$$a_{21} = 1/C_2R_{12}$$

$$a_{22} = a_{21} + a_{23} + b_{22}$$

$$a_{23} = 1/C_2R_{23}$$

$$a_{32} = 1/C_3\ R_{23}$$

$$a_{33} = a_{32} + b_{33}$$

$$b_{11} = 1/C_1R_{F1}$$

$$b_{22} = 1/C_2R_{F2}$$

$$b_{33} = 1/C_3R_{3G}$$

Equations for System Build

$$\dot{T}_1 = -a_{11}T_1 + a_{12}T_2 + b_{11}\ T_{R1}$$

$$\dot{T}_2 = a_{21}T_1 - a_{22}T_2 + a_{23}T_3 + b_{22}\ T_{R2}$$

$$\dot{T}_3 = a_{32}T_2 - a_{33}T_3$$

APPENDIX F
Full Scale Parameters

Characteristic Rates:

$$a_{12} = 0.294$$

$$a_{21} = 0.0144$$

$$a_{23} = 0.01125$$

$$a_{32} = 0.0238$$

$$a_{33} = 0.030$$

$$b_{11} = 0.0563$$

$$b_{22} = 0.037$$

Full Scale Temperatures:

$$T_{R1} = 2670 \text{ K}$$

$$T_{R2} = 2567 \text{ K}$$

LIST OF REFERENCES

1. Nunn, R. H. and Kelleher, M.D., Naval Postgraduate School, Monterey, California, Jet Vane Heat Transfer Modeling, October 1986.

2. Nunn, R. H. Naval Postgraduate School, Monterey, California, TVC Jet Vane Thermal Modeling Using Parametric System Identification, March 1988.

3. Hatzenbuehler, M. A., "Modeling of Jet Vane Heat Transfer Characteristics A Simulation Of Thermal Response", Master's Thesis, U. S. Naval Postgraduate School, Monterey, California, June 1988.

4. Integrated Systems Inc., Palo Alto, California, System Build/PC User's Guide, 1985.

5. Integrated Systems Inc., Palo Alto, California, System ID/PC User's Guide, 1986.

6. Naval Weapons Center, China Lake, California, Retractable Vane Development Test at NWC (Video), RS-670, 22 August 1985 and RS-826, 28 August 1987.

INITIAL DISTRIBUTION LIST

		No. of Copies
1.	Defense Technical Information Center Cameron Station Alexandria, Virginia 22304-6145	2
2.	Library, Code 0142 Naval Postgraduate School Monterey, California 93943-5002	2
3.	Chairman, Code 69 Mechanical Engineering Department Naval Postgraduate School Monterey, California 93943-5002	1
4.	Professor R. H. Nunn, Code 69Nn Mechanical Engineering Department Naval Postgraduate School Monterey, California 93943-5002	5
5.	LT M. M. Reno Naval Amphibious Base, CCU Code OOB Coronado, California 92155-5000	1

Thesis
R3455
c.1

Reno
Modeling transient thermal behavior in a thrust vector control jet vane.